Influence of shear stress applied during flow stoppage and rest period on the mechanical properties of thixotropic suspensions

Guillaume Ovarlez* and Xavier Chateau

Université Paris Est–Institut Navier, Laboratoire des Matériaux et Structures du Génie Civil (LCPC-ENPC-CNRS), 2, Allée Kepler, 77420 Champs-sur-Marne, France

(Received 5 October 2007; published 10 June 2008)

We study the solid mechanical properties of several thixotropic suspensions as a function of the shear stress history applied during their flow stoppage and their aging in their solid state. We show that their elastic modulus and yield stress depend strongly on the shear stress applied during their solid-liquid transition (i.e., during flow stoppage) while applying the same stress only before or only after this transition may induce only second-order effects: there is negligible dependence of the mechanical properties on the preshear history and on the shear stress applied at rest. We also found that the suspensions age with a structuration rate that hardly depends on the stress history. We propose a physical sketch based on the freezing of a microstructure whose anisotropy depends on the stress applied during the liquid-solid transition to explain why the mechanical properties depend strongly on this stress. This sketch points out the role of the internal forces in the colloidal suspensions' behavior. We finally discuss briefly the macroscopic consequences of this phenomenon and show the importance of using a controlled-stress rheometer.

DOI: 10.1103/PhysRevE.77.061403 PACS number(s): 83.80.Hj, 64.70.D−, 83.60.Pq

I. INTRODUCTION

Dense suspensions arising in industrial processes (concrete casting, drilling muds, etc.) and natural phenomena (debris flows) often involve a broad range of particle sizes. The behavior of these materials reveal many complex features which are far from being understood (for a recent review, see Ref. [1]). This complexity originates from the great variety of interactions between the particles (colloidal, hydrodynamic, frictional, collisional, etc.) and of physical properties of the particles (volume fraction, deformability, sensitivity to thermal agitation, shape, buoyancy, etc.) involved in their behavior.

Basically, these materials exhibit a yield stress and have a solid viscoelastic behavior below this yield stress; above the yield stress they behave as liquids: they flow. This yielding behavior originates from the colloidal interactions which create a jammed network of interacting particles [2,3]. These materials also exhibit thixotropic behaviors: their time-dependent properties and the characteristic time to reach a steady state flow depend on the previous flow history [3–5]. Considerable work has been devoted to studying the structure of suspensions under stationary shear flow and its link to the rheological properties of the suspensions (see, e.g., Refs. [1,2,6] for a recent review). It has been well established that the changes in the material properties as a function of the shear history are linked to structural changes. Moreover, when these materials are left at rest (the rest is usually defined as a period characterized by a naught shear rate), their static yield stress τ_c (the shear stress one has to impose to start a flow) increases with the resting time [7–9], and may be one order higher than their dynamic yield stress τ_d (the shear stress for flow cessation). In parallel, the elastic modulus is also found to increase with the resting time [9–11]. These features are shared by many aggregating suspensions and colloidal glasses: in the case of aggregating suspensions, the evolution of the behavior may be explained by a reversible decrease of the flocculation state under shear or an increase if the material is left at rest [12]. In the case of colloidal glasses, the evolution is related to the evolution of the microstructure through a cage-diffusion process [13,14]. In both cases, the evolution at rest is related to Brownian motion of the particles. It is worth noting that physical phenomena that do not occur at the particle scale may also produce mechanical aging. Recently, Manley *et al.* [10] proposed that the mechanical aging of their aggregating suspensions, which is observed without any dynamics at the particle scale, may be attributed to the increase of the contact area between the particles in time.

Applying a given stationary preshear to a thixotropic suspension should enable one to obtain a uniquely defined structure of the material: this structure should depend only on the value of the shear rate applied during the preshear. Then, once the flow is stopped after this given preshear, the mechanical characteristics (elastic modulus and yield stress) of the suspension in its solid state and their evolution at rest would be uniquely determined. However, thixotropic materials may pass from a liquid to a solid state for any stress history below a well defined dynamic yield stress [11]. As far as we know, the effect of the stress history (below the dynamic yield stress) applied during the unsteady flow leading to structural buildup on the structure and the mechanical properties of thixotropic suspensions has not been studied. Moreover, the effect of this stress on the aging of yield stress materials has only been poorly studied.

Recently, Ovarlez and Coussot [15] have shown that when a stress lower that the dynamic yield stress is applied after a strong preshear to a thixotropic suspension in a fully destructured liquid state, its flow stoppage (i.e., its liquid-solid transition) is delayed by a time that increases with the applied stress and diverges at the approach of the dynamic yield stress. They also observed that the elastic modulus of the material once in its solid regime depends on the small stress

*Corresponding author; guillaume.ovarlez@lcpc.fr

(below the dynamic yield stress) that is applied after the preshear. However, they did not focus on this feature.

Cloitre *et al.* [16] have observed that the aging of microgel pastes, as probed by the creep response to a shear stress below the yield stress, gets slower when the applied shear stress is increased. This phenomenon was interpreted as resulting from a competition between aging and partial rejuvenation induced by large rearrangements when the shear stress exceeds a value corresponding to the end of the linear regime of the material. It has also been shown by Viasnoff and Lequeux [17] that the picture may be more complex. They studied the aging of a colloidal suspension through the evolution in time of the microscopic rearrangement kinetics of the particles, probed by diffusing wave spectroscopy. They found that applying oscillations (below the yield strain) to a colloidal suspension at rest may induce either an overaging or a rejuvenation (depending on the strain). Mechanical aging has been observed in frictional materials: the static coefficient of friction increases with the time of rest [18]. This aging, i.e., the increase rate of the static friction coefficient, was found to be strongly accelerated when a stress is applied during rest in solid on solid friction experiments [18] and in granular materials [19–21]. Direct frictional contacts between particles have been proposed to be at the origin of the yield stress [22] and of the mechanical aging [10] of colloidal gels; in this framework, we would thus expect the mechanical aging of such suspensions to be strongly accelerated under stress.

In this paper, we question the influence of the shear stress history under the dynamic yield stress on the solid mechanical properties of thixotropic materials. We control accurately the shear stress imposed during the flow stoppage and the rest of various thixotropic suspensions, and measure their yield stress and elastic modulus evolution in time. We show that their solid mechanical properties depend strongly on the stress applied during their liquid-solid transition (i.e., their flow stoppage), while the stresses applied only before the liquid-solid transition (i.e., during the flow in the liquid state) or only after the liquid-solid transition (i.e., during the aging at rest) may induce only second-order effects. We also show that the suspensions age with a structuration rate that hardly depends on the stress history. The materials and methods used to perform this study are presented in Sec. II. The effect of the stress history on the overall mechanical behavior and on the aging is shown in Sec. III. We discuss the physical origin of the observed behaviors and present some important macroscopic consequences in Sec. IV.

II. MATERIALS AND METHODS

A. Pastes

We perform most experiments on bentonite suspensions. In order to check the generality of our results, we also studied three other thixotropic materials and a simple yield stress fluid: a mustard, a silica suspension, a thixotropic emulsion, and a simple emulsion.

Bentonite suspensions are made of (smectite) clay particles of length of order 1 μm and thickness 10 nm [23]. The particle can aggregate via edge-to-face links, so that the suspension may be seen as a colloidal gel [23]. As a consequence, these suspensions are thixotropic. Moreover, at rest, their yield stress and elastic modulus increase in time. The mechanical properties may be varied by varying the particle volume fraction: we prepare three suspensions, at 6, 9, and 10 % volume fraction, that have an initial (i.e., 100 s after the end of a preshear at high shear rate) static yield stress of 30, 50, and 65 Pa. Each sample was prepared by a strong mixing of the solid phase with water. Then, the suspensions were left at rest for 3 months before any test, which avoids further irreversible (chemical) aging over the duration of the experiments.

The mustard (Maille, France) is a mixture of water, vinegar, mustard seed particles, mustard oil, and various acids. We may see it as a suspension in an oil-in-water emulsion with a large concentration of elements (droplets and particles). The silica suspension is a suspension of silica particles (Rhodia) of 3.7 μm average diameter at a 22% volume fraction; KCl is added at a 0.3 M concentration in order to destabilize the suspension and form a concentrated aggregating suspension.

As a simple emulsion and a thixotropic emulsion, we use the materials of Ragouilliaux *et al.* [24]. The pure emulsion is prepared by progressively adding water in an oil-surfactant solution (Sorbitan monooleate, 2%) under high shear. The water droplets have a 1 μm diameter. Their concentration is fixed at 70%, which means that the droplets are in close contact. This simple emulsion behaves as a simple yield stress fluid (i.e., it exhibits no time dependent behavior). A thixotropic emulsion is made by loading the simple emulsion with colloidal particles [24]. The surfactant and the colloidal particles (hydrophobic clay particles (Bentone 38, Elementis Specialties company) with a mean diameter 1 μm and thickness 10 nm) are first mixed at a solid volume fraction of 3% in the oil; the water is then progressively added in this suspension under high shear. As shown by Ragouilliaux *et al.* [24], this loaded emulsion has a thixotropic behavior. However, this behavior does not originate from the colloidal interactions between the clay particles: the bentonite suspension in oil is a simple fluid. It is thus likely that the clay particles tend to form links between neighboring droplets: the dynamics of these links' formation is at the origin of the thixotropic behavior of the suspension loaded with colloidal particles.

Finally, we have prepared a wide range of materials, from a low volume fraction suspension which may form a loose fractal gel to a dense emulsion in which all droplets are in close contact. The thixotropic and aging behaviors of these materials may have various origins such as aggregation, new link creation between particles in close contact, and rearrangements of the particles' configuration. By performing our experiments on all these materials, we will thus be able to determine whether the behaviors we observe are generic properties shared by thixotropic suspensions, or if they are specific to a given material or a given physical mechanism.

B. Stress histories and rheometrical measurements

Most rheometric experiments are performed within a coaxial cylinder thin gap Couette geometry (inner radius R_i

=17.5 mm, outer cylinder radius R_e=18.5 mm, height H =45 mm) on a commercial rheometer (Bohlin C-VOR 200) that imposes either the torque or the rotational velocity (with a torque feedback). This ensures having a roughly homogeneous stress in the gap. We also checked in a cone and plate geometry (4°, radius 2 cm) that we observe the same phenomena as in the thin gap Couette geometry. In order to avoid wall slip [3], we use sandblasted surfaces of roughness larger than the size of the particles.

1. Procedures

As the materials we study are thixotropic, it is necessary to strongly preshear the materials after loading in order to perform all the measurements in the same conditions, i.e., to start always from a same state of structuration of a material. In all experiments, we thus first preshear the material at high stresses (corresponding to a high shear rate of about 100 s^{-1}) during 200 s in order to start from a fully destructured state of the material in its liquid regime.

After the preshear, we impose various shear stress histories $\tau_0(t)$ below the dynamic yield stress τ_d: the materials may then stop flowing and age at rest under various stresses. Only simple histories in which the stress is piecewise-constant will be considered; the exact procedures will be detailed below (see Fig. 1). In order to study the influence of this shear stress history on the mechanical properties at rest of the materials, we measure the evolution in time of their elastic modulus. We also measure their yield stress as a function of the duration of the stress history $\tau_0(t)$. Before performing the yield stress measurement, we first relax the elastic strain by lowering the stress to 0 Pa during 5 s.

2. Elastic modulus measurements

The evolution in time of the suspensions' elastic modulus is measured by superposing small stress oscillations to the stress history $\tau_0(t)$. We impose $\tau(t)=\tau_0(t)+\delta\tau_0\cos(\omega_0 t)$ and we measure the strain response $\gamma(t)$ $=\gamma_{\text{creep}}(t)+\delta\gamma_0(t)\cos[\omega_0 t+\phi(t)]$. The elastic modulus is then simply $G(t)=\delta\tau_0/\delta\gamma_0(t)$.

In most experiments, the oscillatory shear stress is applied at a frequency of 1 Hz. The amplitude $\delta\tau_0$ depends on the sample: it is chosen so as to ensure that all materials are tested in their linear regime (the strain is always lower than 10^{-3}). These experiments were performed with several different amplitudes on some materials in order to check that the results are independent of the choice of $\delta\tau_0$. We also checked the independence of the results on the frequency; although the overall value of the elastic modulus depends slightly on the frequency, the aging rate and the effect of the stress histories on the mechanical properties we evidence in this paper are not sensitive to the frequency. Finally, we checked that such oscillations do not affect the mechanical properties of the materials: the same elastic modulus is measured after a long time whether oscillations are applied or not during this time. This may seem to be in contradiction with the observations of Viasnoff and Lequeux [17], who found that there is an interplay between the aging and the oscillations, but apart from the differences between their system and ours, it must be noted that they imposed oscillatory

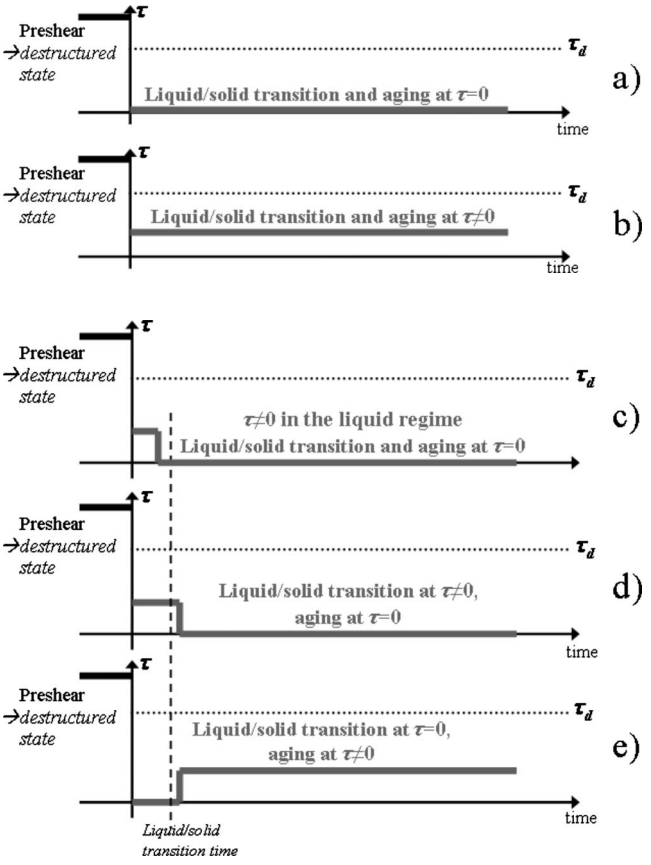

FIG. 1. Shear histories. In all experiments, a strong preshear is first applied to the material in its liquid state. Then (a) a naught shear stress is applied (τ_0=0 Pa); (b) a stress $\tau_0 \neq 0$ Pa lower than the dynamic yield stress τ_d is applied during the liquid-solid transition and all the aging; (c) a stress $\tau_0 \neq 0$ Pa lower than the dynamic yield stress τ_d is applied during flow deceleration as long as the material is in a liquid state, then the stress is lowered to zero during the liquid-solid transition and the aging; (d) a stress $\tau_{\text{transition}} \neq 0$ Pa lower than the dynamic yield stress τ_d is applied during the material liquid-solid transition and then the stress is lowered to zero during the aging; (e) a naught stress is applied during the liquid-solid transition and then a stress $\tau_{\text{aging}} \neq 0$ lower than the dynamic yield stress τ_d is applied during the aging in the solid regime.

strains higher than 2.9% whereas we impose oscillatory strains lower than 0.1%. Actually, from the results of Cloitre *et al.* [16], it seems that probing the material in its linear regime prevents aging from being affected by the oscillations. Note also that as we measure the linearized response of the material around a stress that may be nonzero, we have to check that differences between the elastic moduli measured for various shear stress histories are not due to nonlinear effects. This will be shown in Sec. III A. Note finally that there is a small creep $\gamma_{\text{creep}}(t)$ in response to the applied stress history. As the measurements are performed in the solid regime of the materials, the creep flow is continuously decelerating [11]. In all the experiments we performed, except during the first few seconds after imposing τ_0, the creep rate $\dot{\gamma}_{\text{creep}}(t)$ was always $<10^{-4}$ s^{-1} so that there was no interplay between the negligible creep and the elasticity measurement.

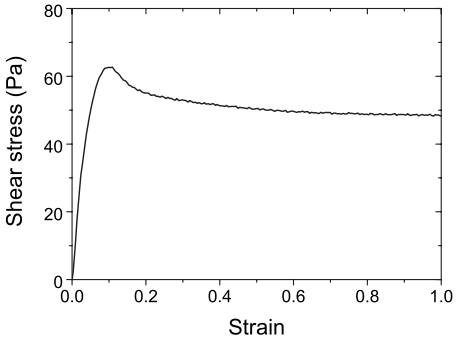

FIG. 2. Shear stress vs strain when slowly shearing a 9% bentonite suspension from rest at 10^{-2} s^{-1}, 600 s after the end of the preshear.

3. Yield stress measurements

We mainly perform our yield stress measurements by means of a velocity controlled method [25]: the inner cylinder is driven at a low velocity, and the yield stress is defined by the overshoot presented by the shear stress in a shear stress vs strain plot (see an example in Fig. 2 for a 9% bentonite suspension). This yields a good evaluation of the yield stress as the overshoot is followed by a slow stress decrease: this means that the material starts to be destructured at the overshoot (as long as the shear time scale is lower than the structuration time scale) and thus flows. Note that, as the materials we study are thixotropic, the value of the yield stress depends on the time elapsed between the end of the preshear and the measurement: this resting time must then be controlled. We chose to drive the inner cylinder in order to induce a shear rate of 0.01 s^{-1}. We checked that the features we observe in this paper do not depend on the low shear rate that is imposed to measure the yield stress. We finally checked that our results are independent of the measurement procedure: we also performed linear shear stress ramps [26]; in these experiments the shear stress is increased linearly in time and is plotted vs the shear rate in order to identify the value of the shear stress at the onset of flow [27].

III. EXPERIMENTAL RESULTS

Let us first show the impact of applying a constant stress τ_0 below the dynamic yield stress τ_d to a thixotropic suspension after a preshear [procedures of Figs. 1(a) and 1(b)]. In Fig. 3(a) we plot the elastic modulus of a 9% bentonite suspension vs the time elapsed since the end of the preshear, for $\tau_0=0$ Pa and $\tau_0=22$ Pa. In both cases, the elastic modulus G' increases in time. This is characteristic of the aging at rest of thixotropic materials [9,11]. However, depending on the applied shear stress τ_0, we observe striking differences in the behavior at short times. While the elastic modulus G' increases regularly from time $t=0$ s when a zero shear stress is applied after the preshear, when a nonzero shear stress τ_0 is applied, G' is equal to zero (within the measurement uncertainty) in a first stage and it suddenly starts increasing at some time $t_{\text{transition}} \neq 0$ (here equal to 19 s for $\tau_0=22$ Pa). Afterwards, we see that both moduli increase regularly in time, with roughly the same increase rate. However, at a given time, the modulus measured when a stress $\tau_0 \neq 0$ is applied is much higher than the modulus observed at zero stress: here, for $\tau_0=22$ Pa, G' is 600 Pa higher than for $\tau_0=0$ Pa. As G' is measured as the linearized response of the material to oscillations around different τ_0 in these experiments, we checked that differences between the elastic moduli measured with both procedures are not due to nonlinear effects: we showed that the same modulus is measured around $\tau_0 \neq 0$ as the one measured around 0 Pa when removing the stress τ_0 after a long time.

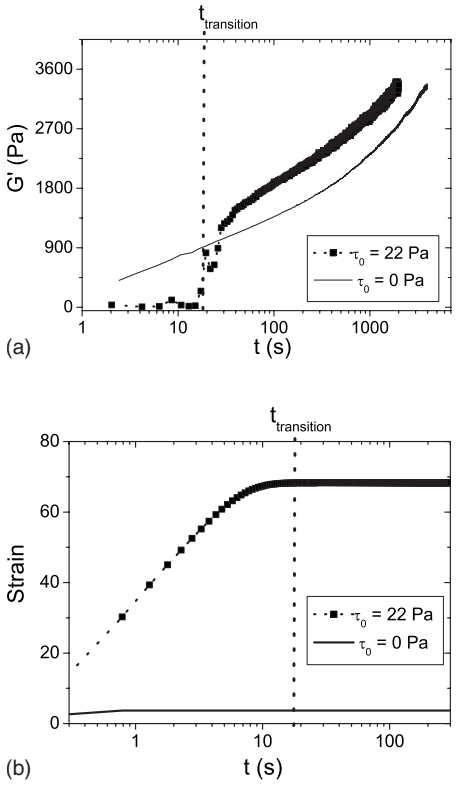

FIG. 3. (a) Elastic modulus G' vs time t after strongly shearing a 9% bentonite suspension, for two different stresses applied after the preshear [see Figs. 1(a) and 1(b)]: $\tau_0=0$ Pa (line) and 22 Pa (squares). (b) Strain vs time after strongly shearing a 9% bentonite suspension, for the same experiments as in Fig. 3(a) (by convention the strain is chosen as 0 at $t=0$ s). The vertical dotted line delimits the liquid and solid regimes of the bentonite suspension in the experiment performed at $\tau_0=22$ Pa, and defines the liquid-solid transition time $t_{\text{transition}}$.

In the following, we first show that the sudden increase in time of the elastic modulus we observe for $\tau_0 \neq 0$ is the signature of a liquid-solid transition. We then show that the large difference in the elastic modulus values observed for different τ_0 is due mainly to the stress applied during this liquid-solid transition. We also show that the stress applied only during the flow before stoppage and during the aging in the solid state have basically no influence on the mechanical properties. We finally quantify the link between the applied stress at the liquid-solid transition and the increase of the elastic modulus and the yield stress of the materials. We study the behavior of the bentonite suspensions in detail and show that these features are shared by all the thixotropic materials we studied.

A. Liquid-solid transition

As shown in detail by Ovarlez and Coussot [15], the sudden appearance of an elastic behavior in colloidal suspensions observed in Fig. 3 is the signature of a liquid-solid transition of the material. Superposition of oscillations to a constant shear stress actually allows us to identify unambiguously the liquid and the solid states of thixotropic materials [15]. The constant stress probes the flow properties, while the superimposed small oscillations probe the actual material strength. In Fig. 3(b) we plot the strain response to the constant stress vs time after the same stress step as in the experiments of Fig. 3(a); by convention the strain is chosen as 0 at $t=0$ s. We observe that, when a stress $\tau_0=0$ Pa is applied, the flow stops within a few 100 ms (due to fluid inertia) corresponding to a strain of around 3.7, whereas when a stress $\tau_0=22$ Pa is applied, the strain increases during around 20 s, resulting in a strain of order 70; afterwards, the strain saturates. Consistently, the beginning of the plateau of strain corresponds to the sudden appearance of a substantial elastic modulus in the material. This indicates that the material is now in a solid state, while it was in a liquid state during its flow. Finally, these observations allow us to identify precisely and unambiguously the liquid regime (the material flows and has a negligible elastic modulus) and the solid regime (the material stops flowing and gets a substantial elastic modulus) of the material. As shown by Ovarlez and Coussot [15], this identification of the liquid and solid regimes is consistent with the loss modulus G'' measurements: G'' is larger than the elastic modulus G' and is proportional to the apparent viscosity of the material during the flow; at the liquid-solid transition, G'' starts to decrease while G' abruptly increases and crosses over the G'' curve at its peak. The liquid-solid transition occurs after a time $t_{\text{transition}}$ (equal to 19 s in Fig. 3) that increases with τ_0, and which tends to infinity when τ_0 tends to a stress τ_d (see Ref. [15]), i.e., the material remains indefinitely in a liquid state for $\tau_0 > \tau_d$: this defines precisely τ_d as the dynamic yield stress.

In the following, we thus redefine the relevant aging time as the time spent by the material in its solid regime: $t_{\text{aging}}=t-t_{\text{transition}}(\tau_0)$. The G' data of Fig. 3(a) are replotted vs t_{aging} in Fig. 4. Both elastic moduli now seem to increase at the same rate during the whole aging time and to differ basically only by a constant value $\Delta G'$ (here around 600 Pa) that may depend on τ_0. We investigate the origin of these moduli differences on the stress history in the following.

B. Influence of the stress history

It is known that the structure and the steady state flow properties of suspensions depend on their shear history. It is thus first worth wondering if the effect we observe is the consequence of a dependence on the applied stress of the structural buildup in the liquid regime before flow stoppage. Moreover, as stated in the Introduction, a stress applied on a solid aging material may be expected to change its behavior. We can then also wonder if the effect we observe is the consequence of a dependence on the applied stress of the structural evolution of the material. That is why we study the impact on the mechanical properties of the stress applied

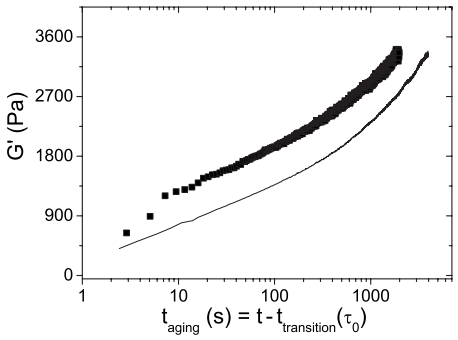

FIG. 4. Same data as in Fig. 3(a) plotted vs the time spent in the solid regime $t_{\text{aging}}=t-t_{\text{transition}}(\tau_0)$.

during these three phases: the shear flow in the liquid regime, the liquid-solid transition, and the aging in the solid regime. In order to separate the effects of the applied stress in these three phases, we have applied the following stress histories [see Figs. 1(c)–1(e)], in complement to the simple stress histories of Figs. 1(a) and 1(b).

In a first series of experiments [Fig. 1(c)], after a preshear, we apply a nonzero stress $\tau_0 < \tau_d$ during a time $t_0 < t_{\text{transition}}(\tau_0)$ just too short for the liquid-solid transition to occur, before relaxing the stress to zero during the liquid-solid transition and the aging at rest; we then measure the elastic modulus and yield stress evolution in time. These experiments test the influence of the stress applied in the liquid regime.

In a second series of experiments [Fig. 1(d)], just after the preshear we impose a nonzero stress $\tau_{\text{transition}} < \tau_d$ during a time sufficient for the material to stop flowing and pass from a liquid to a solid state under this stress. Afterwards, we apply no stress during the aging ($\tau_{\text{aging}}=0$ Pa) and we measure the elastic modulus and yield stress evolution in time. When compared with the experiment of Fig. 1(c), these experiments test the influence of the stress applied during the liquid-solid transition.

In a third series of experiments [Fig. 1(e)], just after the preshear we first impose a naught stress during a time $t_{\text{stop}}=30$ s sufficient for the material to pass from a liquid to a solid state and then we impose a nonzero stress $\tau_{\text{aging}} < \tau_d$ during the aging in the solid state; we then measure the elastic modulus and yield stress evolution in time. These experiments test the influence of the stress applied during the aging in the solid state. The elastic modulus measurements performed on the 9% bentonite suspension with the procedures of Figs. 1(a)–1(e) are plotted vs time in Fig. 5.

1. Impact of the stress applied in the liquid regime

Importantly, with the procedure of Fig. 1(c), we found that when applying $\tau_0 \neq 0$ only during a time too short for the liquid-solid transition to occur (here this time was chosen as 14 s), the elastic modulus value and its evolution in time are the same as when $\tau_0=0$ Pa during the whole experiment (Fig. 5). The conclusion is that there is no significant dependence of the elastic modulus on the shear history in the liquid regime before flow stoppage. We checked this feature for several values of τ_0. This means that while the intensity of

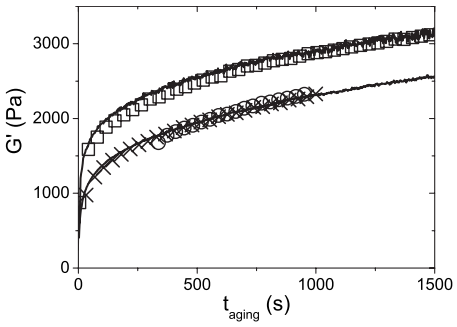

FIG. 5. Elastic modulus G' vs time after strongly shearing a 9% bentonite suspension, measured with the various procedures of Fig. 1: (a) when a stress $\tau_0=0$ Pa is applied during the whole experiment (lower line); (b) when a stress $\tau_0=22$ Pa is applied during the whole experiment (upper line); (c) when a stress $\tau_0=22$ Pa is applied during $t_0=14$ s ($t_0<t_{\text{transition}}$) and then lowered to zero during the liquid-solid transition and the aging (crosses); (d) when a liquid-solid transition stress $\tau_{\text{transition}}=22$ Pa is applied during $t_0=22$ s ($t_0>t_{\text{transition}}$) and then lowered to zero during the aging (empty squares); (e) when a liquid-solid transition stress $\tau_{\text{transition}}=0$ Pa is applied during 30 s and then an aging stress $\tau_{\text{aging}}=22$ Pa is applied during 300 s (empty circles).

the shear may probably influence the material state, as shown by many authors for steady-state flows [6], it is clearly not at the origin of the strong elastic modulus strengthening we evidence here (note that the shear rate value just before lowering τ_0 to 0 Pa in Fig. 5 was of order 0.1 s^{-1} whereas it is of order 100 s^{-1} during the preshear). Compared with what we observe, the shear history in the liquid regime may induce only second-order effects on the solid mechanical properties of the suspensions.

We also checked that the intensity of the preshear applied before lowering the stress below τ_d has no influence on the results. Finally, we have performed experiments in which the stress $\tau_{\text{transition}}$ is applied in the direction opposite to the preshear. The results, presented in Fig. 8(a), show that the same result is obtained whatever the relative direction of the preshear and of $\tau_{\text{transition}}$. This means that, while it is known that a preshear in a given direction creates an anisotropic microstructure [28,29], the impact of this anisotropy on the solid mechanical properties is negligible or erased by the shear stress history applied after the preshear.

2. Impact of the stress applied during the liquid-solid transition

In order to evaluate the impact of the stress applied during the liquid-solid transition of the material, we plot in Fig. 5 the elastic modulus vs time for the procedure depicted in Fig. 1(d) applied to the 9% bentonite suspension: a stress $\tau_0=22$ Pa is first applied during a time $t_0=22$ s just longer than the liquid-solid transition time $t_{\text{transition}}=19$ s before being lowered to zero. We observe that the elastic modulus value and its evolution in time are exactly the same as when a stress $\tau_0=22$ Pa is applied during the whole experiment. This result, together with the observation that the stress applied only while the material is in a liquid state has basically no influence on the elastic modulus value, means that the material state is changed only by the stress applied during the very short moment during which the material passes from a liquid to a solid state. The strain of a few unities during which this liquid-solid transition occurs is enough to induce the effect we observe. Afterwards, when the material is in a solid state, this stress can be removed with no consequence: the material has been irreversibly changed. It also shows that the differences we observe in the mechanical behavior as a function of the stress τ_0 do not simply reflect a nonlinear elastic behavior: when $\tau_{\text{transition}}=22$ Pa, the same elastic modulus is observed whether it is measured around 0 Pa or around 22 Pa during the aging (Fig. 5).

3. Impact of the stress applied during the aging in the solid state

Another important consequence of obtaining the same results with the procedures of Figs. 1(b) and 1(d) is that maintaining the stress τ_0 during the whole aging after the liquid-solid transition does not enhance the strengthening of the material. In other words, once the material has been changed during the liquid-solid transition, there is no stress-induced accelerated aging.

The material state thus seems to depend only on the stress applied during the liquid-solid transition. However, another possibility is that applying a shear stress at any time during rest in the solid state may lead to the same consequence: once the material is in its solid regime, the stress may induce a reorganization of the material structure that modifies its mechanical state once and for all. This can be checked with the procedure of Fig. 1(e), where the liquid-solid transition occurs under a zero stress whereas a stress $\tau_{\text{aging}}\neq 0$ is applied once the material is in its solid state. For the sake of simplicity, we consider only stress histories in the solid regime leading to a small creep flow, ensuring that the material stays in a solid state. As the yield strain of the suspension is of order 0.1 (see Fig. 2) a small creep flow is defined here as a creep flow of strain less than 0.05. As the static yield stress of the materials we study increases with the resting time (see below), such simple histories can be achieved by applying the aging stress τ_{aging} only after a long enough resting time (whose value depend on the stress and the material) at $\tau_0=0$ Pa. In Fig. 5 we plot the elastic modulus vs time when first applying a stress $\tau_{\text{transition}}=0$ Pa during 30 s and then a stress $\tau_{\text{aging}}=22$ Pa during 300 s (leading to a creep flow of strain 0.03). With this procedure, we find that the same modulus is measured when no stress is applied during both the liquid-solid transition and the aging, as when a stress $\tau_{\text{aging}}\neq 0$ is applied only once the material is in its solid state. This finally shows that there is no stress-induced accelerated mechanical aging in solid materials obtained with $\tau_{\text{transition}}=0$ Pa.

We observe the same features in Fig. 6 on a 6% bentonite suspension, with the procedures of Figs. 1(a), 1(b), 1(d), and 1(e). We first recover that the elastic modulus is higher when $\tau_{\text{transition}}\neq 0$ than when $\tau_{\text{transition}}=0$ Pa. We then recover that the same result is obtained when applying a stress $\tau_0\neq 0$ during both the liquid-solid transition and the aging, and during the liquid-solid transition only. We also recover that the material behavior is basically the same when no stress is applied during both the liquid-solid transition and the aging

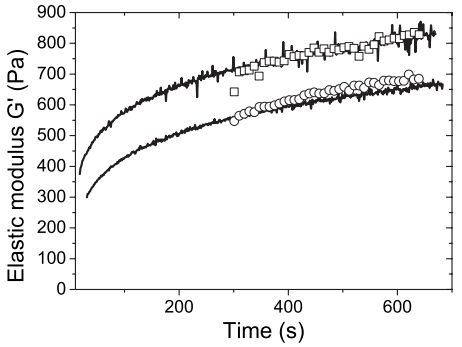

FIG. 6. Elastic modulus vs time after strongly shearing a 6% bentonite suspension, measured with the various procedures of Fig. 1: when a stress $\tau_0=0$ Pa is applied during the whole experiment (lower line); when a stress $\tau_0=7$ Pa is applied during the whole experiment (upper line); when a liquid-solid transition stress $\tau_{transition}=7$ Pa is applied during 30 s and then lowered to zero during the aging (empty squares); when a liquid-solid transition stress $\tau_{transition}=0$ Pa is applied during 100 s and then an aging stress $\tau_{aging}=7$ Pa is applied during 200 s (empty circles).

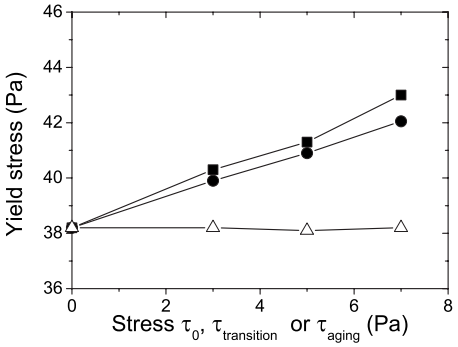

FIG. 7. Yield stress 300 s after strongly shearing a 6% bentonite suspension, vs τ_0, $\tau_{transition}$, or τ_{aging}, for the various procedures of Fig. 1: when a stress τ_0 ranging between 0 and 7 Pa is applied (squares) during the whole experiment; when a liquid-solid transition stress $\tau_{transition}$ ranging between 3 and 7 Pa is applied during 30 s and then removed (circles); when a liquid-solid transition stress $\tau_{transition}=0$ Pa is applied during 100 s and then an aging stress τ_{aging} ranging between 3 and 7 Pa is applied during 200 s (open triangles).

as when a stress $\tau_{aging} \neq 0$ is applied only once the material is in a solid state. These results confirm that what matters is actually the stress that is applied during the liquid-solid transition: this stress only is at the origin of the strengthening of the material in its solid state. The stress applied during the aging has basically no influence on the solid mechanical state of the material.

Note that stress histories applied after the liquid transition leading to a more important creep flow were found to lead to more complex histories whose analysis is out of the scope of the present paper. When such a stress history is applied to the material, after the liquid-solid transition that occurs under a naught stress, one first observes a solid-liquid transition induced by the applied stress and then a second liquid-solid transition. The stress that is applied during these phases may then have an impact on the material state because it is applied during a new liquid-solid transition.

4. Impact of the stress history on the static yield stress

We also observe that the static yield stress depends on the shear stress history applied below the dynamic yield stress: if a constant stress is applied after the preshear, the yield stress is higher than when no stress is applied (Fig. 7). The yield stress measurements performed on a 6% bentonite suspension with the procedures of Figs. 1(a), 1(b), 1(d), and 1(e) are presented vs the stress applied during the liquid-solid transition and/or the aging in Fig. 7, for a total aging time in the solid regime of 300 s. As observed for the elastic modulus measurements, we find that the same result is obtained when applying a shear stress τ_0 during both the liquid-solid transition and the aging and during the liquid-solid transition only. Moreover, when the aging stress τ_{aging} is not applied during the liquid-solid transition but only once the material is in a solid state, then the yield stress is the same as when no stress is applied during aging. This shows that, as for the elastic modulus, the yield stress enhancement is induced only by the stress applied during the liquid-solid transition. The stress applied during the aging has basically no influence on the solid mechanical state of the material.

5. Summary

To sum up, we have observed that the overall mechanical behavior of a bentonite suspension depends strongly on the stress $\tau_{transition}$ applied during its liquid-solid transition: the material is strengthened when a nonzero $\tau_{transition}$ is applied. On the other hand, we observed basically no dependence on the shear history in the liquid regime nor on the stress applied at rest. What matters is thus applying a stress to the material during the few seconds after the preshear during which a liquid-solid transition occurs, until it is in a solid state. Then this stress can be removed with no consequence: the material has been irreversibly changed. We also found that the materials age, but, surprisingly, we found that the mechanical aging kinetics (G' evolution in time) is basically unchanged by the stress history.

C. Constitutive laws accounting for the liquid-solid transition stress

In the following, most results were obtained using the procedure of Fig. 1(d), i.e., a shear stress $\tau_{transition}$ is applied during the liquid-solid transition and is removed during the aging of the material; the elastic modulus evolution in time is then measured around a naught stress. Afterwards, the yield stress is measured as a function of the time t_{aging} spent by the materials in their solid regime. The elastic modulus measurements are performed on all the materials presented in Sec. II A; the yield stress measurements are performed only on the bentonite suspensions.

1. Elastic modulus

In Figs. 8(a), 9(a), and 10(a), we plot the elastic modulus values vs the time spent in the solid regime for different values of $\tau_{transition}$ applied during the liquid-solid transition,

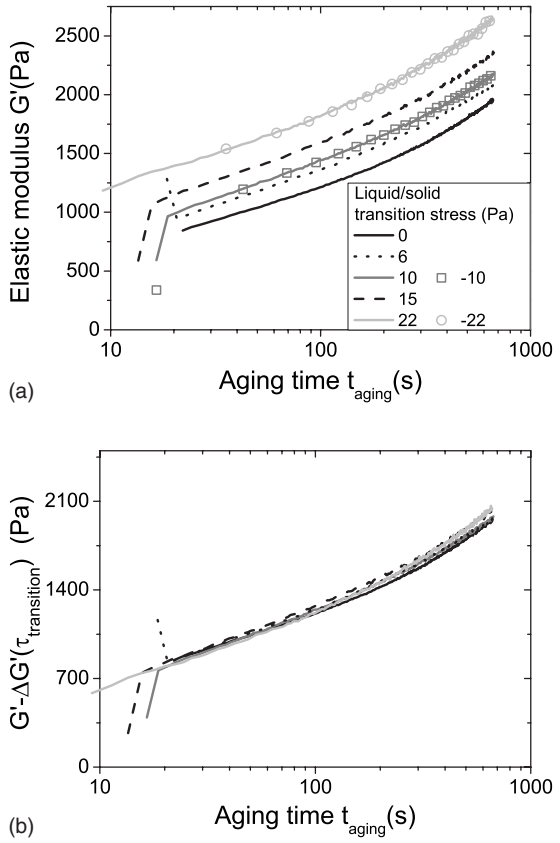

FIG. 8. (a) Elastic modulus vs time after strongly shearing a 9% bentonite suspension, measured around 0 Pa for various stresses $\tau_{\text{transition}}$ applied during the liquid-solid transition (a negative value of $\tau_{\text{transition}}$ represents a stress applied in the direction opposite to the preshear direction). (b) Same data as in Fig. 8(a), when the elastic modulus is shifted by a constant value $\Delta G'(\tau_{\text{transition}})$ (see Fig. 11).

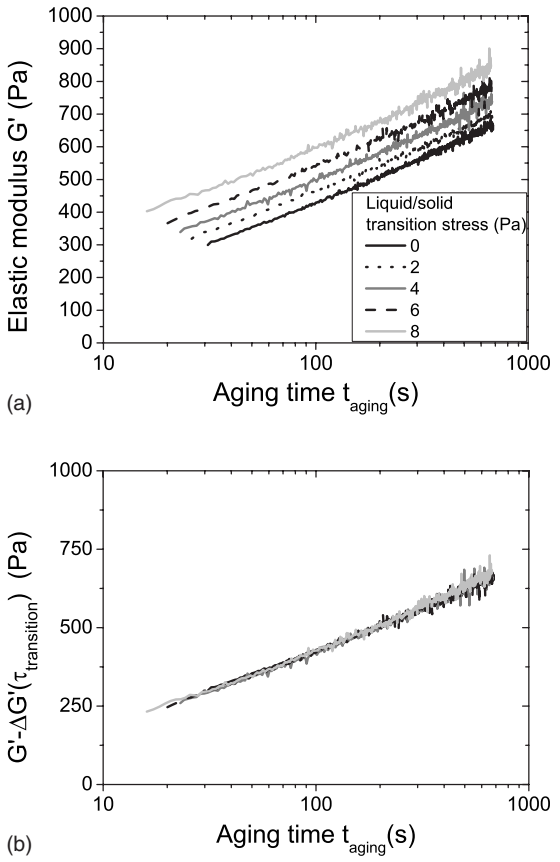

FIG. 9. Same plots as in Fig. 8 for a 6% bentonite suspension.

for three different bentonite suspensions. For all materials, we notice that the elastic modulus is strongly increased by the stress that is applied during the liquid-solid transition. For example, in Fig. 10(a), we see that the elastic modulus measured after a 100 s aging time increases from 1400 to 3000 Pa when $\tau_{\text{transition}}$ is changed from 0 to 40 Pa. However, surprisingly, as noticed in Sec. III A, we observe that the aging kinetics seems to be basically unchanged by this stress. The elastic modulus value $G'(t_{\text{aging}}, \tau_{\text{transition}})$ as a function of the time t_{aging} spent in the solid regime and of the stress $\tau_{\text{transition}}$ applied during the liquid-solid transition would then read

$$G'(t_{\text{aging}}, \tau_{\text{transition}}) = G'_0(t_{\text{aging}}) + \Delta G'(\tau_{\text{transition}}). \quad (1)$$

In Figs. 8(b), 9(b), and 10(b), we now plot the elastic modulus values shifted by constant values $\Delta G'(\tau_{\text{transition}})$ vs the time spent in the solid regime for the same data as in Fig. 8(a), 9(a), and 10(a). We observe a rather good superposition of all data; there may be, however, a small discrepancy beyond a 15 min aging time as seen in Fig. 10(b), but at this stage this is a second-order effect. The $\Delta G'(\tau_{\text{transition}})$ values for all $\tau_{\text{transition}}$ values on all materials are plotted in Fig. 11.

We observe that, for a given material, $\Delta G'(\tau_{\text{transition}})$ increases linearly with $\tau_{\text{transition}}$. However, writing

$$\Delta G'(\tau_{\text{transition}}) = \alpha \tau_{\text{transition}} \quad (2)$$

we see that there is no universal value of α. α seems to depend on the clay particles' volume fraction: we find α values between 20 and 40. It is still possible that the relevant scaling is $\Delta G'(\tau_{\text{transition}})/G'_m \approx \lambda \tau_{\text{transition}}/\tau_m$, with λ a universal constant, and with G'_m and τ_m mechanical characteristics of the materials: τ_m may then be the dynamic yield stress, but, as the materials age, we did not find how to define a characteristic elastic modulus G'_m, therefore we could not test such a scaling.

In order to show that the phenomenon we observe here is not specific to bentonite suspensions, but is a general phenomenon occurring in a wide range of thixotropic materials, we performed the same experiments (although in a less detailed way) on a mustard, a silica suspension, and a thixotropic emulsion (see Sec. II A). The results of the procedures of Figs. 1(a) and 1(b) are depicted in Fig. 12.

We observe that, as in the bentonite suspensions, the elastic modulus values of the mustard, the silica suspension, and the thixotropic emulsion strongly increase when a stress $\tau_{\text{transition}}$ is applied during the liquid-solid transition. We checked that the same result is recovered when the stress is applied only during the liquid-solid transition as when it is applied during both the liquid-solid transition and the aging. We also observe in Fig. 12 that the aging kinetics is basically unmodified by the applied stress (there may be a very small

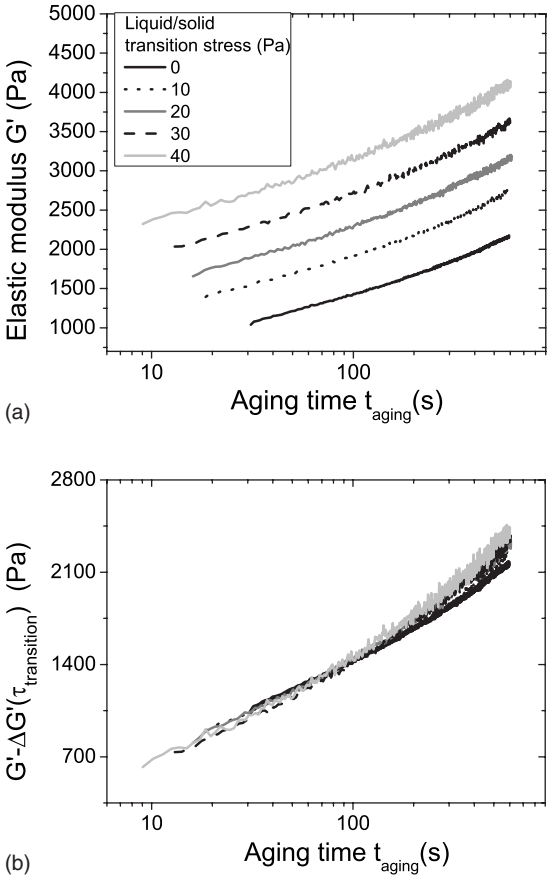

FIG. 10. Same plots as in Fig. 8 for a 10% bentonite suspension.

increase of the elastic modulus increase rate of the silica suspension and the thixotropic emulsion for high stresses, but we did not study this effect and it is clearly a second-order effect). The effect of $\tau_{\text{transition}}$ on the quantitative increase of the elastic modulus of these materials is depicted in Fig. 11: it is of the same order as in the bentonite suspensions, and it is consistent with Eq. (2). However, the α parameter of Eq. (2) is of the order of 80 for the silica suspension whereas it is of order 16 for the mustard, and of order 7 for the thixotropic emulsion showing again that this parameter is material dependent.

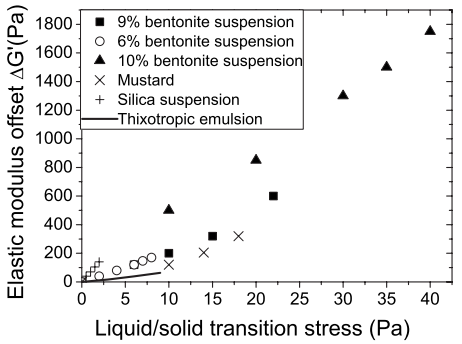

FIG. 11. Elastic modulus offset $\Delta G'(\tau_{\text{transition}})$ obtained by superposing the data of Figs. 8 (squares), 9 (open circles), 10 (triangles), 12(a) (crosses), and 12(b) (pluses) vs the stress $\tau_{\text{transition}}$ applied during the liquid-solid transition.

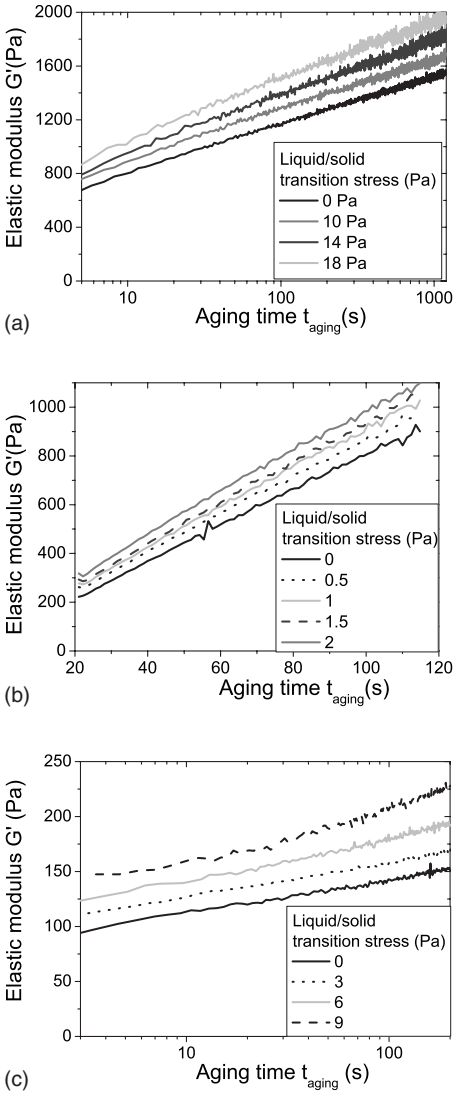

FIG. 12. (a) Elastic modulus vs time for various stresses $\tau_0 < \tau_d$ applied after strongly shearing a mustard. (b) Elastic modulus vs time for various stresses $\tau_0 < \tau_d$ applied after strongly shearing a silica suspension. (c) Elastic modulus vs time for various stresses $\tau_0 < \tau_d$ applied after strongly shearing a thixotropic emulsion.

Finally, we performed the same experiments on a simple (nonthixotropic) emulsion. In contrast with what is observed in the loaded emulsion, we found that elastic modulus of the simple emulsion has the same value whatever the stress $\tau_{\text{transition}}$. It shows that the effect we observe is certainlyspecific to thixotropic materials, and it points out the role of the dynamics of link creation between the particles.

2. Yield stress

In Fig. 13, we present the yield stress values measured on a 9% bentonite suspension for various stresses $\tau_{\text{transition}}$ ranging between 0 and 22 Pa, and for various aging times. In Fig. 13, we observe that the yield stress is strongly increased by the stress $\tau_{\text{transition}}$ that is applied during the liquid-solid transition. However, as already noticed in Sec. III A for the elastic modulus measurements, we observe that the aging kinet-

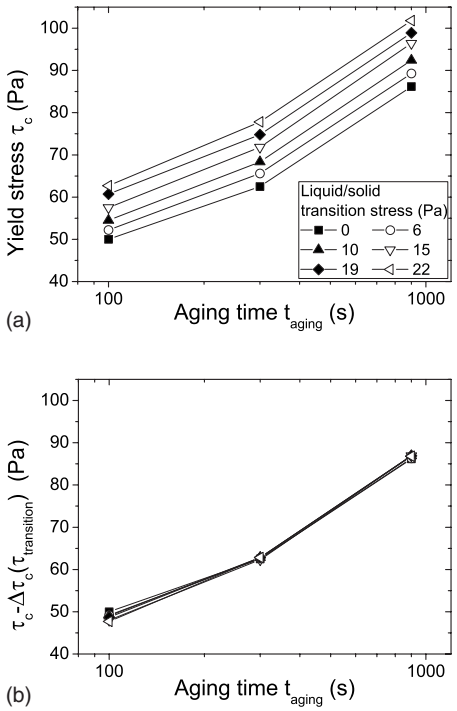

FIG. 13. (a) Yield stress τ_c vs time after strongly shearing a 9% bentonite suspension, for various stresses $\tau_{transition}$ applied during the liquid-solid transition. (b) Same data as in Fig. 13(a), when the yield stress is shifted by a constant value $\Delta\tau_c(\tau_{transition})$.

ics seems to be unchanged by this stress. The yield stress value $\tau_c(t_{aging}, \tau_{transition})$, as a function of the time t_{aging} spent in the solid regime and of the stress $\tau_{transition}$ applied during the liquid-solid transition, would then just be shifted by a constant $\Delta\tau_c(\tau_{transition})$ value and read

$$\tau_c(t_{aging}, \tau_{transition}) = \tau_{c_0}(t_{aging}) + \Delta\tau_c(\tau_{transition}). \quad (3)$$

We performed the same experiments on the two other bentonite suspensions and observed the same features: all results are in agreement with Eq. (3). The stress offsets $\Delta\tau_c(\tau_{transition})$ for all bentonite suspensions are presented in Fig. 14.

We observe in Fig. 14 that the stress shift $\Delta\tau_c(\tau_{transition})$ increases linearly with $\tau_{transition}$. However, writing

$$\Delta\tau_c(\tau_{transition}) = \beta\tau_{transition} \quad (4)$$

we see, as for the elastic modulus measurements, that there is no universal value of β. β seems to depend slightly on the material: we find β values between 0.6 and 0.9.

It is worth noting that the phenomenon we observe is not an artifact of the yield stress measurement procedure: we checked that the same phenomenon, with the same quantitative effect, is observed with another yield stress measurement method, based on a shear stress ramp [26,27]. Finally, note that measuring the yield stress by imposing a slow velocity in the opposite direction to the preshear yields a slightly higher value than measuring this yield stress in the same direction as the preshear. This is due to a shear-induced anisotropy of the suspensions [28,29]. However, we checked that the effect of $\tau_{transition}$ is to increase the yield stress by the same amount whatever the relative directions of the preshear and the yield stress measurement. This indicates that the yield surface is increased isotropically rather than shifted.

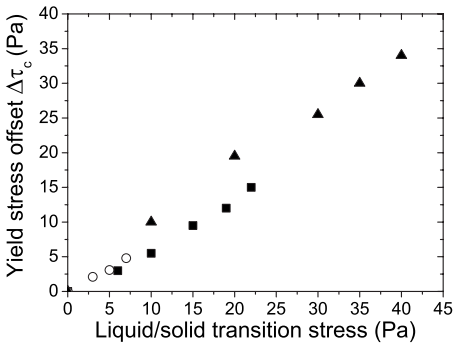

FIG. 14. Yield stress offset $\Delta\tau_c(\tau_{transition})$ obtained by superposing the data of Fig. 13 for a 9% bentonite suspension (squares), and for the same experiments on a 6% (open circles) and a 10% (triangles) bentonite suspension vs the stress $\tau_{transition}$ applied during the liquid-solid transition.

IV. DISCUSSION

A. Interpretation

In order to account for all the observations we made in Sec. III, we need to find a structuration mechanism that (i) depends on the shear stress $\tau_{transition}$ applied at the transition between the liquid and the solid regimes so that different initial solid mechanical states are created by different $\tau_{transition}$, (ii) is consistent with the mechanical properties being shifted by a value roughly proportional to $\tau_{transition}$ [Eqs. (2) and (4)], (iii) is consistent with a structuration rate (the increase rate of their elastic modulus and yield stress) basically independent of the stress history, and (iv) is consistent with the different microstructures of the various suspensions we study.

Point (i) can be easily understood. It is well known that a flow induces an anisotropic microstructure in suspensions of colloidal and noncolloidal particles [28,29], and that the degree of anisotropy increases with the shear rate as a result of a competition between Brownian motion (that tends to isotropize the microstructure) and hydrodynamic interactions [30]. Here, we face complex suspensions that jam rapidly when the applied stress is lower than the dynamic yield stress τ_d. We can plausibly propose that if this structuration occurs while a stress is applied to the material, different microstructures are frozen during the liquid-solid transition depending on $\tau_{transition}$. As the mechanical properties of suspensions depend on their microstructure [31], these materials then have naturally different elastic moduli. However, it is important to note that the solid mechanical properties of the materials depend mainly on the stress applied at the liquid-solid transition, while there is basically no influence of the shear history in the liquid regime. This would mean that even if the flow induces a microstructure anisotropy, this anisotropy is likely to disappear quickly if the stress is removed before the liquid-solid transition, due to Brownian motion of the particles in the liquid state. A key point thus seems that

this anisotropy is frozen at the liquid-solid transition thanks to the stress that is applied during this transition. Actually, the particle positions in the disordered particle network that is frozen must be compatible with the stress applied during the transition. This means that, depending on this stress, preferential orientations of the pair forces are chosen to ensure this compatibility. In the Appendix, leaving aging apart, we present a sketch of a simple 2D model colloidal suspension in order to present how such a mechanism may work. Through a micromechanical analysis of the behavior of this model suspension, we simply draw the consequences of the existence of repulsive and attractive forces in the suspension. Then, within this picture, we show that a jamming at a given $\tau_{\text{transition}}$ may induce a change in the microstructure that actually implies a roughly linear dependence of the effective elastic modulus on $\tau_{\text{transition}}$.

The role of aging: As regards the mechanism of aging, it should first be noted that the observation of similar evolution in time of the moduli of materials for different $\tau_{\text{transition}}$ would mean that although these materials behave differently on the mechanical point of view, the underlying physical mechanism of their aging is the same and is at the same stage at a same given aging time t_{aging}. Then, the requirement (iii) that the increase rate of the mechanical properties is basically independent of τ_{aging} is important and discriminating. It seems that the energy landscape visited during the aging is unaffected by the shear stress applied during aging in our systems, and that a model of aging based on stress-biased energy barriers [18] would fail to describe our systems. This is thus probably neither consistent with models based on the aging at the contact scale [10] nor with models in which the yield stress originates from the static friction between the particles [22] as it was observed in several systems that the aging of solid contacts is very sensitive to the shear stress applied during aging [18–21]. This feature actually requires an aging mechanism that is basically insensitive to the stress transmitted in the solid network. We think that this is consistent with a structure buildup due to creation of new contacts between particles, leading to strengthening of the material. In this case, once the material is in a solid state, we can think that the stress τ_{aging} is transmitted only by the solid skeleton: the free particles (or aggregates) in the suspension that stick on this skeleton thanks to Brownian motion are then insensitive to the applied stress. As a consequence, the further increase of the elastic modulus due to the new links that are created would be independent of the stress τ_{aging} applied during the aging.

B. Macroscopic consequences

From a practical point of view, our results point out the importance of well controlled experimental conditions for performing yield stress measurements. On the one hand, the yield stress at which a flow stops (the dynamic yield stress τ_d) is well defined from creep tests [11]: starting from a fully destructured liquid state of a material, if a creep stress above τ_d is prescribed then the material flows steadily whereas for a creep stress below τ_d there is a creep flow that is slowing down at any time and the strain rate tends toward 0. On the other hand, we have observed a feature: the yield stress at which the flow starts (the static yield stress τ_c) is not uniquely defined: it depends strongly on the stress applied during the liquid-solid transition.

As a consequence, if one just pours a material in a cup to perform a measurement, how it was poured, i.e., how its flow stopped, may have an influence on the yield stress that is measured. Nevertheless, in order to avoid irreproducible material preparation and to perform measurements on a well defined state, one usually preshears the material, and then stops shearing the material during a given resting period before performing the yield stress measurement. However, an important difference remains between different measurement methods. This difference stands in what is called "rest": a material is said to be at rest when it is not flowing. With a stress-controlled rheometer, the rest is imposed by applying a stress $\tau_0=0$ Pa; as we have shown in this paper, this yields a well defined unique solid state. With a rate-controlled rheometer, after a preshear at a given $\dot{\gamma}_p$, the rest is defined by $\dot{\gamma}_{\text{rest}}=0\ \text{s}^{-1}$ (i.e., the tool rotation is abruptly stopped) so that the stress state during the liquid-solid transition and rest is not *a priori* known. As we have shown that the static yield stress actually depends on this stress, this implies that the initial state of the material is ill defined in such experiments. This ill definition of the initial state can be seen in papers showing raw data of yield stress measurements performed with the vane method (see, e.g., Fig. 4 of Ref. [32] and Fig. 9 of Ref. [33]): in this case, it is observed that the stress at the beginning of the measurement is different from zero, which means that the material was stressed during the flow stoppage and the rest. This feature may explain partly the differences between measurements performed with stress-controlled rheometers and strain-controlled rheometers, and between different groups in Ref. [34] on the same materials. This shows that stress-controlled rheometers, or rate and stress-controlled rheometers, are preferable for well-defined yield stress measurements: an appropriate resting period should be defined as a period during which a stress $\tau_0=0$ Pa is applied rather than a shear rate $\dot{\gamma}_{\text{rest}}=0\ \text{s}^{-1}$.

While our paper was under review, we read a preprint [35] that shows results that may be consistent with ours on a colloidal gel. In this preprint, Osuji *et al.* [35] found that when the flow of their system is stopped at $\dot{\gamma}=0\ \text{s}^{-1}$ after a strong preshear at 10^2–$10^3\ \text{s}^{-1}$, the elastic modulus G' at rest is higher for a higher intensity of preshear. They attributed this increase to the dependence of the fractal structure on the shear stress τ_{preshear} applied during the preshear. However, they also noticed that the elastic modulus is linearly correlated with what they call "residual" or "internal" stress τ_{internal}, namely, the stress resulting from the rapid quench in the solid regime when applying abruptly $\dot{\gamma}=0\ \text{s}^{-1}$ at the end of the preshear. We think that τ_{internal} is nothing else than our liquid-solid transition stress $\tau_{\text{transition}}$ which is here uncontrolled because of the use of a velocity-controlled mode to stop the shear. We suggest that the relationship found by Osuji *et al.* [35] between G' and τ_{preshear} may be fortuitous and simply due to the fact that for a given τ_{preshear}, they have a given uncontrolled $\tau_{\text{transition}}$ (or equivalently τ_{internal}) upon imposing $\dot{\gamma}=0\ \text{s}^{-1}$. We also suggest that the relationship between G' and $\tau_{\text{transition}}$ (or τ_{internal}) is more relevant. This can be easily proved by varying independently τ_{preshear} and

$\tau_{transition}$, i.e., by working with a stress controlled mode, at least for flow stoppage.

This phenomenon may also explain the discrepancy between classical rheometrical measurements and inclined plane measurements with the method of Coussot *et al.* [8], performed on the same materials by Nguyen *et al.* [34] (see Fig. 9 of Ref. [34]). Coussot *et al.* [8] proposed to first pour the material on an inclined plane at a given slope in order to measure its dynamic yield stress (from the final height of the deposit), and then to incline further the plane in order to measure its static yield stress (from the angle of the plane at flow restart). Our experiments show that this method is incorrect: when the flow stops on the inclined plane, the stress at the base of the material is equal to its dynamic yield stress: the liquid-solid transition then occurs under a nonzero shear stress. The static yield stress of the material measured afterwards is then higher than what it would be if the liquid-solid transition had occurred under a zero shear stress. Moreover, as the stress increases from bottom to top in the layer, the solid material is heterogeneous: its actual yield stress increases from bottom to top. We will present a detailed study of this problem, as well as a relevant method to measure correctly the yield stress in an inclined plane experiment in a future work [27].

More generally, the way the flow is stopped before a yield stress measurement should depend on the practical application that is of interest: in problems where one seeks for the restart of a flow after an abrupt flow cessation, it is of importance to know how the previous flow actually stopped. For example, in pipe flows such as concrete pumping or in extrusion processes, which are often rate controlled through the action of a piston, the stress at a flow cessation is likely to be near the dynamic yield stress: the flow will then be harder to restart than what would be expected from a rheometrical measurement performed with $\tau_{transition}=0$ Pa. On the other hand, in applications where the material passes from a liquid to a solid state under a naught shear stress then the relevant yield stress is the one measured with $\tau_{transition}=0$ Pa. This is the case, e.g., when a material is poured in its liquid state in a receptacle: in this case, the liquid material is in a hydrostatic stress state when it passes from a liquid to a solid state. An example of such a situation is given by thixotropic concrete casting in formwork: in order to predict the stresses supported by the walls after concrete casting, one needs the static yield stress of the material [36], which is given in this case by the one measured with $\tau_{transition}=0$ Pa; we actually showed that the yield stress of thixotropic cement pastes involved in concrete mix design strongly depends on $\tau_{transition}$ [37].

Finally, it should be stated that for complex flow histories, a given material stops under a heterogeneous stress distribution: this yields to a material of heterogeneous mechanical properties. Any flow restart may then happen with a complex yield surface [27].

V. CONCLUSION

We have studied the mechanical aging at rest of several different thixotropic colloidal suspensions, under various shear stress histories applied during their flow stoppage and their aging in their solid state. We have shown that their solid mechanical properties depend strongly on the shear stress applied while they pass from a liquid to a solid state (i.e., during flow stoppage). Basically, we found that the elastic modulus and the yield stress increase linearly with the shear stress applied at the liquid-solid transition. On the other hand, we have shown that there is negligible dependence of these mechanical properties on the preshear history and on the shear stress applied at rest. Compared with the impact of the shear stress applied at the liquid-solid transition, applying the same stress only before or only after the liquid transition may induce only second-order effects on the solid mechanical properties. Moreover, the elastic modulus and the yield stress of thixotropic suspensions at rest increase in time, but we have observed that the structuration rate (the increase rate of the elastic modulus and the yield stress) hardly depends on the stress history. We showed that the phenomenon we evidence in this paper may reflect the differences in the microstructures that are frozen at the liquid-solid transition. A micromechanical analysis of the behavior of a 2D model colloidal suspension, with repulsive and attractive pair interactions, allowed us to show that a jamming at a given $\tau_{transition}$ may induce a change in the microstructure that implies a roughly linear dependence of the effective elastic modulus on $\tau_{transition}$. This points out the role of the internal forces in the colloidal suspensions' behavior. The independence of the increase rate of the mechanical properties on the stress applied during aging may require an aging mechanism that is insensitive to the stress transmitted in the solid network: this is consistent with a structure buildup through new contact creation. We have also shown that these results may have important macroscopic consequences. This tells us how careful rheometrical tests must be designed to measure correctly the static yield stress; in particular, one would better control the shear stress applied at flow stoppage. Moreover, in any practical case, this implies that the threshold for flow initiation as well as the yield surface in the material depend a lot on how the flow was stopped.

ACKNOWLEDGMENTS

We thank Philippe Coussot, Anaël Lemaître, and Nicolas Roussel for many fruitful discussions throughout this work. Special thanks to Alexandre Ragouilliaux for providing the thixotropic and simple emulsions. Support from the Agence Nationale de la Recherche (ANR) is acknowledged (Grant No. ANR-05-JCJC-0214).

APPENDIX: IMPACT OF THE LIQUID-SOLID TRANSITION STRESS IN A SIMPLE SKETCH OF A COLLOIDAL SUSPENSION

In the following, we present a simple model of a colloidal suspension, in order to show how a liquid-solid transition occurring at a given $\tau_{transition}$ may induce a change in the microstructure that implies a roughly linear dependence of the effective elastic modulus on $\tau_{transition}$. Of course, this model is not intended to be a model of the systems we study experimentally; moreover, note that we do not attempt to

describe the evolution in time of the microstructure in the solid regime. We intentionally stay at a conceptual level as our aim is not to explain and account for the time-dependent properties of materials. It is just a simple colloidal model system that allows us to draw the consequences of the existence of interaction forces at a macroscopic level, and to show that a simple micromechanical analysis is able to account for the effect we observe (independently of any aging feature). Of course, in order to model our experimental systems, we would have to add complexity in the model in order to take into account spatial heterogeneities, aging, etc. But these last features, as we show in the following, are not necessary to explain the observation of the phenomenon we evidence: the key point is the existence of internal forces in the suspension.

Our model colloidal suspension is a bidimensional monodisperse suspension of particles distributed in an incompressible Newtonian fluid. The particles interact through pair colloidal interactions involving both attractive and repulsive forces [31]. We focus on the mechanical behavior at the liquid-solid transition: in this case, the suspension is at rest and the hydrodynamic interactions are negligible. We consider cases where the interaction forces dominate the Brownian effect. Then, the particles form a disordered network and the contribution of the fluctuations to the stress tensor can be neglected. For the sake of simplicity, it is assumed (i) that all the repulsive forces (all the attractive forces) have same intensity equal to f_a ($f_r>0$), and (ii) that the distance between two interacting particles is equal to l_a (l_r) when the force is attractive (repulsive).

Let us consider a representative elementary volume V of the suspension, large enough to be of typical composition. If the 2D colloidal network is at rest, the macroscopic Cauchy stress tensor reads [31,38,39]

$$\sigma_{xx} = \frac{1}{|V|}\int_{-\pi/2}^{\pi/2} [f_a l_a p_a(\theta) - f_r l_r p_r(\theta)]\cos^2\,\theta d\theta,$$

$$\sigma_{yy} = \frac{1}{|V|}\int_{-\pi/2}^{\pi/2} [f_a l_a p_a(\theta) - f_r l_r p_r(\theta)]\sin^2\,\theta d\theta,$$

$$\sigma_{xy} = \frac{1}{|V|}\int_{-\pi/2}^{\pi/2} [f_a l_a p_a(\theta) - f_r l_r p_r(\theta)]\cos\,\theta \sin\,\theta d\theta, \tag{A1}$$

where θ denotes the angular position of the vector joining two interacting particles with respect to the x axis, $|V|$ is the area of the domain V, and $p_a(\theta)d\theta\,[p_r(\theta)d\theta]$ is the number of attractive (repulsive) doublets located in the representative elementary volume, of orientation belonging to $[\theta, \theta+d\theta]$.

The overall behavior of the suspension is determined in the framework of a mean-field approach. Then, when a small macroscopic shear strain γ is prescribed to the representative elementary volume, the variation of the distance between two particles interacting through an attractive potential reads $\frac{dl_a}{l_a} = \gamma \cos\,\theta \sin\,\theta$. Of course, the same relation holds for a repulsive doublet.

If k_a (k_r) denotes the rigidity associated to the attractive (repulsive) potential when the distance between the particles is equal to l_a (l_r), then the variation of the elastic energy stored in the representative elementary volume associated with the overall shear deformation is the sum of the variation of elastic energy stored in all the doublets, which reads

$$dW = \frac{1}{|V|}\int_{-\pi/2}^{\pi/2}\left[\left(f_a dl_a + \frac{1}{2}k_a dl_a^2\right)p_a(\theta) + \left(f_r dl_r + \frac{1}{2}k_r dl_r^2\right)p_r(\theta)\right]d\theta. \tag{A2}$$

The overall behavior of the suspension being elastic, Eq. (A2) also reads $dW=\tau\gamma+\frac{1}{2}G\gamma^2$, where τ denotes the overall shear stress (below the yield stress) applied to the unstrained suspension and G the macroscopic shear modulus in the xy direction. This finally yields the following expression for the macroscopic shear modulus:

$$G = \frac{1}{|V|}\int_{-\pi/2}^{\pi/2} [k_a l_a^2 p_a(\theta) + k_r l_r^2 p_r(\theta)]\cos^2\,\theta \sin^2\,\theta d\theta. \tag{A3}$$

Let us now show that in this simple model colloidal suspension, the behavior observed in our experiments is recovered. First, let $p_a^0(\theta)$ and $p_r^0(\theta)$ denote the angular repartition of the doublets in the solid state when no stress is applied during the liquid-solid transition. The two functions $p_a^0(\theta)$ and $p_r^0(\theta)$ have to ensure that the three integrals of Eq. (A1) are naught. The value of the shear modulus G_0 corresponding to this case is obtained by putting $p_a^0(\theta)$ and $p_r^0(\theta)$ into Eq. (A3).

Many solutions for the orientation distribution of the doublets exist so that Eqs. (A1) are satisfied. We do not need at this stage to make any assumption on this distribution: it is not necessarily isotropic. On the other hand, when a shear stress $\tau_{\text{transition}}$ is applied during the liquid-solid transition, it is assumed that some of the doublets change their orientation so that Eqs. (A1) hold with $\sigma_{xy}=\tau_{\text{transition}}$, while all the other quantities describing the morphology of the suspension at the particle scale $(l_r, l_a, f_r, f_a, k_r, k_a)$ remain unchanged.

In our picture, the distribution of orientation frozen at the liquid-solid transition is modified if $\tau_{\text{transition}} \neq 0$. We choose to describe the modified distributions of orientation for the doublets by

$$p_a(\theta) = p_a^0(\theta) - \frac{n_a}{\pi} + n_a\delta(\theta - \pi/4),$$

$$p_r(\theta) = p_r^0(\theta) - \frac{n_r}{\pi} + n_r\delta(\theta + \pi/4), \tag{A4}$$

where n_a (n_r) denotes the number of attractive (repulsive) doublets that change their orientation with respect to the distribution defined by $p_a^0(\theta)$ $[p_r^0(\theta)]$, and $\delta(\theta)$ is the Dirac distribution. The new distribution of attractive doublets is obtained from the original one by assuming that n_a doublets, initially uniformly distributed in space, rotate from their original position to the position defined by $\theta=\pi/4$. The same

phenomena occur for n_r repulsive doublets rotating from their original orientation to the position $\theta=-\pi/4$. These preferential directions are chosen consistently with what is observed under shear [28–30].

Putting Eqs. (A4) into Eqs. (A1) yields the stress tensor value at the liquid-solid transition in this simple picture

$$\sigma_{xx}=\sigma_{yy}=0, \quad \sigma_{xy}=\tau_{\text{transition}}=\frac{1}{2|V|}(f_a l_a n_a + f_r l_r n_r), \tag{A5}$$

i.e., there is a direct link between the number of doublets that change their orientation to preferential directions and $\tau_{\text{transition}}$ which is the stress at the liquid-solid transition. On the other hand, from Eqs. (A4) and (A3), the elastic modulus reads

$$G=G_0+\frac{1}{8|V|}[k_a(l_a)^2 n_a + k_r(l_r)^2 n_r], \tag{A6}$$

i.e., the elastic modulus is increased by a quantity proportional to the number of doublets changing their orientation. From Eqs. (A5) and (A6), it is thus clearly seen that $\Delta G(\tau_{\text{transition}})$ is roughly proportional to $\tau_{\text{transition}}$, and exactly proportional in some particular cases. If, e.g., $n_a=n_r$, we have

$$G-G_0=\frac{1}{4}\frac{k_a(l_a)^2+k_r(l_r)^2}{f_a l_a + f_r l_r}\tau_{\text{transition}}, \tag{A7}$$

where

$$\frac{k_a(l_a)^2+k_r(l_r)^2}{f_a l_a + f_r l_r} > 0.$$

To sum up, within this simple picture of a 2D model colloidal suspension with repulsive and attractive pair interactions, we have shown that a liquid-solid transition under a stress $\tau_{\text{transition}} \neq 0$ implies a particle pair change of orientation that yields an increase of the elastic modulus roughly proportional to $\tau_{\text{transition}}$.

[1] J. J. Stickel and R. L. Powell, Annu. Rev. Fluid Mech. **37**, 129 (2005).
[2] R. G. Larson, *The Structure and Rheology of Complex Fluids* (Oxford University Press, New York, 1999).
[3] P. Coussot, *Rheometry of Pastes, Suspensions and Granular Materials* (Wiley, New York, 2005).
[4] K. Dullaert and J. Mewis, J. Rheol. **49**, 1213 (2005).
[5] J. Mewis, J. Non-Newtonian Fluid Mech. **6**, 1 (1979).
[6] J. Vermant and M. J. Solomon, J. Phys.: Condens. Matter **17**, R187 (2005).
[7] D. C. H. Cheng, Rheol. Acta **25**, 542 (1986).
[8] P. Coussot, Q. D. Nguyen, H. T. Huynh, and D. Bonn, J. Rheol. **46**, 573 (2002).
[9] C. Derec, G. Ducouret, A. Ajdari, and F. Lequeux, Phys. Rev. E **67**, 061403 (2003).
[10] S. Manley *et al.*, Phys. Rev. Lett. **95**, 048302 (2005).
[11] P. Coussot, H. Tabuteau, X. Chateau, L. Tocquer, and G. Ovarlez, J. Rheol. **50**, 975 (2006).
[12] F. Pignon, A. Magnin, and J. M. Piau, J. Rheol. **42**, 1349 (1998).
[13] B. Abou, D. Bonn, and J. Meunier, Phys. Rev. E **64**, 021510 (2001).
[14] D. Bonn, H. Tanaka, G. Wegdam, H. Kellay, and J. Meunier, Europhys. Lett. **45**, 52 (1999).
[15] G. Ovarlez and P. Coussot, Phys. Rev. E **76**, 011406 (2007).
[16] M. Cloitre, R. Borrega, and L. Leibler, Phys. Rev. Lett. **85**, 4819 (2000).
[17] V. Viasnoff and F. Lequeux, Phys. Rev. Lett. **89**, 065701 (2002).
[18] P. Berthoud, T. Baumberger, C. G'Sell, and J. M. Hiver, Phys. Rev. B **59**, 14313 (1999).
[19] W. Losert, J. C. Géminard, S. Nasuno, and J. P. Gollub, Phys. Rev. E **61**, 4060 (2000).
[20] F. Restagno, C. Ursini, H. Gayvallet, and E. Charlaix, Phys. Rev. E **66**, 021304 (2002).
[21] G. Ovarlez and E. Clément, Phys. Rev. E **68**, 031302 (2003).
[22] E. M. Furst and J. P. Pantina, Phys. Rev. E **75**, 050402(R) (2007).
[23] P. F. Luckham and S. Rossi, Adv. Colloid Interface Sci. **82**, 43 (1999).
[24] A. Ragouilliaux, G. Ovarlez, N. Shahidzadeh-Bonn, B. Herzhaft, T. Palermo, and P. Coussot, Phys. Rev. E **76**, 051408 (2007).
[25] Q. D. Nguyen and D. V. Boger, J. Rheol. **27**, 321 (1983).
[26] P. H. T. Uhlherr, J. Guo, C. Tiu, X. M. Zhang, J. Z. Q. Zhou, and T. N. Fang, J. Non-Newtonian Fluid Mech. **125**, 101 (2005).
[27] G. Ovarlez and N. Roussel (unpublished).
[28] C. Mathis, G. Bossis, and J. F. Brady, J. Colloid Interface Sci. **126**, 16 (1988).
[29] F. Parsi and F. Gadala-Maria, J. Rheol. **31**, 725 (1987).
[30] D. R. Foss and J. F. Brady, J. Fluid Mech. **407**, 167 (2000).
[31] W. B. Russel, D. A. Saville, and W. R. Schowalter, *Colloidal Dispersions* (Cambridge University Press, Cambridge, 1995).
[32] Q. D. Nguyen and D. V. Boger, J. Rheol. **29**, 335 (1985).
[33] A. E. James, D. J. A. Williams, and P. R. D. Williams, Rheol. Acta **26**, 437 (1987).
[34] Q. D. Nguyen, T. Akroyd, D. C. De Kee, and L. Zhu, Korea-Aust. Rheol. J. **18**, 15 (2006).
[35] C. O. Osuji, C. Kim, and D. A. Weitz, e-print arXiv:0710.0042v1.
[36] G. Ovarlez and N. Roussel, Mater. Struct. **37**, 269 (2006).
[37] G. Ovarlez and N. Roussel, in *Self-Compacting Concrete—SCC 2007, Proceedings of the Fifth International RILEM Symposium, Ghent, Belgium*, edited by G. De Schutter and V. Boel (Ghent University Press, Ghent, Belgium, 2007).
[38] G. K. Batchelor, J. Fluid Mech. **41**, 545 (1970).
[39] X. Chateau, P. Moucheront, and O. Pitois, J. Eng. Mech. **128**, 856 (2002).